Please cite this article in press as: Albert et al., The Resting Human Brain and Motor Learning, Current Biology (2009), doi:10.1016/j.cub.2009.04.028

Current Biology *19*, 1–5, June 23, 2009 ©2009 Elsevier Ltd All rights reserved DOI 10.1016/j.cub.2009.04.028

Report

The Resting Human Brain and Motor Learning

Neil B. Albert,[1,2] Edwin M. Robertson,[3] and R. Chris Miall[1,*]
[1]Behavioural & Brain Sciences Centre
School of Psychology
University of Birmingham
Birmingham B155 2TT
UK
[2]Department of Psychology
University of Chicago
5848 S. University Ave.
Green Hall 317
Chicago, IL 60637
USA
[3]Berenson-Allen Center for Non-Invasive Brain Stimulation
Harvard Medical School, Beth Israel Deaconess Medical Center
330 Brookline Ave.
Kirstein Building KS 221
Boston, MA 02215
USA

Summary

Functionally related brain networks are engaged even in the absence of an overt behavior. The role of this resting state activity, evident as low-frequency fluctuations of BOLD (see [1] for review, [2–4]) or electrical [5, 6] signals, is unclear. Two major proposals are that resting state activity supports introspective thought or supports responses to future events [7]. An alternative perspective is that the resting brain actively and selectively processes previous experiences [8]. Here we show that motor learning can modulate subsequent activity within resting networks. BOLD signal was recorded during rest periods before and after an 11 min visuomotor training session. Motor learning but not motor performance modulated a fronto-parietal resting state network (RSN). Along with the fronto-parietal network, a cerebellar network not previously reported as an RSN was also specifically altered by learning. Both of these networks are engaged during learning of similar visuomotor tasks [9–22]. Thus, we provide the first description of the modulation of specific RSNs by prior learning—but not by prior performance—revealing a novel connection between the neuroplastic mechanisms of learning and resting state activity. Our approach may provide a powerful tool for exploration of the systems involved in memory consolidation.

Results and Discussion

Motor Performance and Motor Learning

To measure the modulation of resting state activity after a short period of sensorimotor learning, we exposed two groups of participants to one of two versions of a visuomotor "center-out" tracking task [23] (Figure 1A; see Supplemental Experimental Procedures available online). The test group (n = 12) adapted their joystick movements to a novel relationship between cursor and joystick (motor learning), whereas the control group (n = 12) performed similar tracking movements but with veridical cursor feedback of the joystick (motor performance).

In the test group, the movement of the cursor relative to the joystick was gradually rotated about the center of the screen, increasing by 10° each minute (dashed line, Figure 1B). Thus both groups began the task with 0° perturbation and their performance was initially comparable (see Supplemental Results, Behavioral Results). But during the remaining 10 min, the movements of the test group clearly reflected their progressive compensation for the visuomotor perturbation. By the end of the visuomotor task, the mean joystick direction for the test group was rotated by 58.7° with respect to the target direction (black line, Figure 1B). This level of adaptation, compensating for 65% of the imposed perturbation, is similar to performance observed in other experiments (see also Supplemental Experimental Procedures, Behavioral Protocols) (e.g., [24, 25]).

Model-Free Whole-Brain Probabilistic Independent Components Analysis

Probabilistic independent components analysis (PICA) of the BOLD signal allowed us to identify the networks evident during rest [26] and to measure changes in these components after motor learning (test group, n = 12) or motor performance (control group, n = 12). We contrasted the engagement of these networks identified by PICA before ($REST_1$) and after ($REST_2$) the visuomotor task. To ensure that the second resting period was not affected by perseverating on the motor task, we preceded each rest period by a 4 min "dummy" task, in which the subjects observed point light displays of human movements or scrambled dots (Figure 1A; see Experimental Procedures for details).

Baseline Analysis

To first check comparable baseline activity in the two groups, $REST_1$ data for both groups were combined in a single PICA analysis with a between-groups contrast. This concatenation of data across participants allows the PICA analysis to identify spatially consistent regions across the groups that are correlated in their BOLD signal activity, but without the constraint that the activity in individual participants is temporally correlated with other participants or with any external stimulus time course [26]. We identified six previously reported RSNs (see Figures 2A–2E and 2H of [4]). None of these components significantly varied between groups during the initial resting session (each $t(22) < 0.56$, each $p > 0.29$).

Analysis of Learning-Dependent Change

The BOLD data from both sessions ($REST_1$ and $REST_2$) were then analyzed for each group (test and control) independently, testing for RSN components that changed in strength after motor learning (in the test group) or motor performance (in the control group). In the test group, a fronto-parietal (Figure 2) and a cerebellar (Figure 3) component were reliably identified across both REST sessions and significantly increased in strength after motor learning. In the control group, the fronto-parietal component (but not the cerebellar component)

*Correspondence: r.c.miall@bham.ac.uk

Please cite this article in press as: Albert et al., The Resting Human Brain and Motor Learning, Current Biology (2009), doi:10.1016/j.cub.2009.04.028

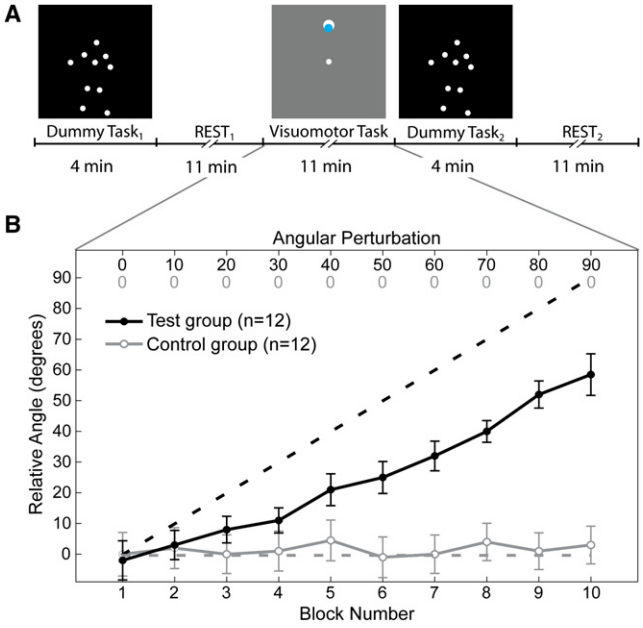

Figure 1. Experimental Design and Performance during the Visuomotor Task

(A) The experiment began with a dummy task and a baseline rest condition ($REST_1$, 11 min) followed by the visuomotor task (11 min). Then participants completed a second dummy task before the final rest condition ($REST_2$, 11 min). The dummy task display was of point light displays of human whole-body movements, or scrambled versions that showed the same individual dot motions, but with random positions. The visuomotor task display shows the central start location, a target and the cursor.

(B) In the visuomotor task the relative angle of the cursor motion compared to the joystick gradually increased with each block, for the test group (dashed group), but remained veridical for the control group. The mean direction of joystick movement with respect to the target (solid line, ±1 SEM) steadily increased for the test group (black) and remained constant for the control group (gray).

was reliably identified in both rest sessions, and this component did not change in strength after the visuomotor task. This increase in component strength reflects an increase in the BOLD signal variability that can be attributed to a particular component.

The fronto-parietal component included the prefrontal cortex, the superior and inferior parietal cortex, and Crus II of the cerebellum (see Table S1). This component was reliable across both rest sessions in the test group ($z = 1.91$, $p = 0.028$; Figure 2A) and across both rest sessions in the control group ($z = 1.65$, $p = 0.01$; Figure 2C), but only changed from $REST_1$ to $REST_2$ in the test group (i.e., after motor learning; $t(11) = 2.074$, $p = 0.031$; Figure 2B). The fronto-parietal component had also been reliably identified in our baseline analysis comparing $REST_1$ data between the two groups (Figure S1A; $z = 2.28$, $p = 0.01$), and its baseline activity was not significantly different between groups (Figure S1B; $t(22) = -0.42$, $p = 0.34$). Thus, the fronto-parietal component, though similar in both groups during the initial resting scan, was altered only after learning.

Additionally, a component that encompassed the majority of the cerebellum was identified in the analysis across both rest sessions in the test group (Figure 3A; $z = 1.78$, $p = 0.038$), and this component also significantly increased after learning the novel motor skill ($t(11) = 1.880$, $p = 0.043$; Figure 3B). This component had not been identified in our combined baseline (i.e., test and control group) analysis of $REST_1$, however, suggesting that it may be qualitatively different from conventional RSNs. No other components were identified by the PICA analysis that significantly increased or decreased in strength between $REST_1$ and $REST_2$.

The ICA approach identifies regions with correlated patterns of resting activity. To explore whether the learning-dependent changes we identified have additional, within-component structure, we additionally performed within-subject, within-session whole-brain correlations against the time-course of BOLD signal recorded within small "seed" regions of interest (see Table S1). The 48 resulting covariance maps for each seed ROI (2 groups of 12 subjects, two sessions) were then tested for significant group × session interactions. Detailed description is beyond the scope of this short report, but we found significant group × session interactions between (1) inferior frontal gyrus, middle frontal gyrus, and cerebellar lobule IX, (2) superior frontal gyrus and fusiform cortex, (3) the angular gyrus and hippocampus, and (4) the precentral gyrus and the middle frontal gyrus and inferior frontal cortex (see Supplemental Results). Thus the main group × session interactions are within the components identified by the

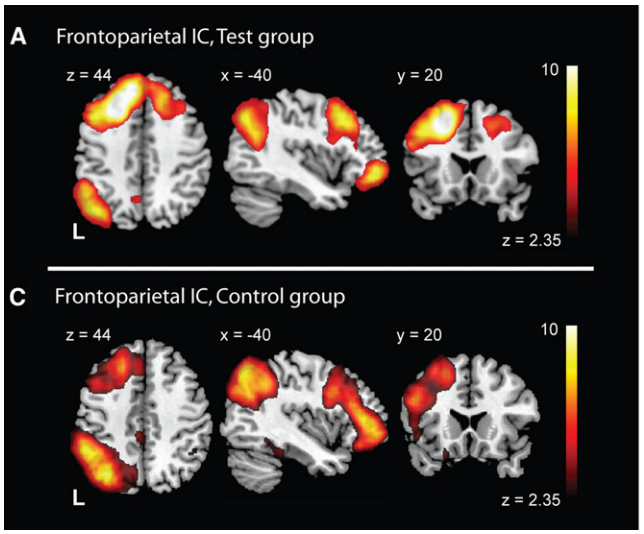

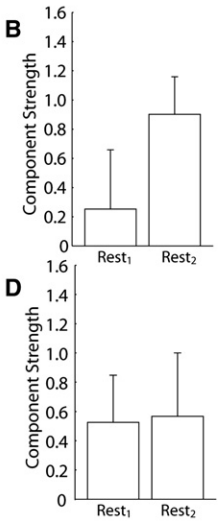

Figure 2. A Fronto-Parietal Resting State Network that Increased in Strength after Exposure to the Visuomotor Adaptation, but Not Performance

This independent component was identified as reliable across the participants in each group and across both rest blocks. The fronto-parietal network (A, C) closely corresponds to a previously identified RSN [3, 4]. The strength of the fronto-parietal network during rest was increased after motor learning (B), but not after motor performance (D).

Please cite this article in press as: Albert et al., The Resting Human Brain and Motor Learning, Current Biology (2009), doi:10.1016/j.cub.2009.04.028

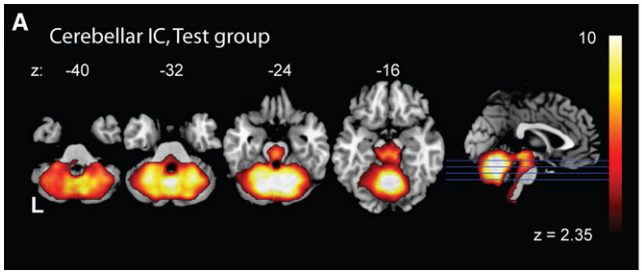

Figure 3. Resting State Activity within the Cerebellum Increased in Strength after Exposure to the Visuomotor Adaptation Task

This independent component (A) was reliably identified across the combined data for both rest sessions in the test group across, and significantly differed between the two rests (B). The absence of this network in previous reports on resting state networks and its absence in the control group suggests that activation of this network may have been driven by the motor learning experience.

PICA analysis; however, there are small but significant regions lying outside of the fronto-parietal and cerebellar components that are affected by motor learning.

Our results demonstrate that motor learning, but not motor performance, modulates subsequent resting activity in specific task-relevant networks. The fronto-parietal network was identified in both groups within their initial resting brain activity (see Figure S1) but was modulated in the test group only after the acquisition of a novel motor skill (see Figure 2). In contrast, when there was no motor skill to learn (i.e., in the control group), there was no change in the spontaneous activity after motor performance. Thus, neuroplastic changes, driven by learning a novel motor skill, shaped subsequent spontaneous activity within the resting brain. This demonstrates a link between neuroplastic processing and resting brain activation, which has implications for both our understanding of memory processing and the functional interpretation of resting brain activity.

Changes in resting state activity were induced specifically by learning. The tasks performed by the two groups were virtually identical, with the exception that the test group learned to compensate for gradually shifting visuomotor feedback. We found no evidence of any change in movement direction, peak velocity, or latency in the control group, and the performance measure of interest—the direction of their joystick motion—was stable throughout. Accordingly, the significant changes observed in the two resting state components in the test group (Figures 2 and 3) are attributable to learning. This is an important distinction from an earlier report of offline persistence of memory-related activity [27]. That work was not able to test whether the activity measured in an auditory oddball task, modulated by exposure to one of two different learning tasks, was influenced by task performance or by learning.

Changes in resting activity were not limited to the time immediately after learning, but were measured after conscious processing has been redirected to an unrelated dummy task for a period of 4 min. Consequently, our results should not be confounded by processing attributable to ruminating about the tracking task. This is a critical feature of the data reported here, because the persistence of neural activity across unrelated tasks would be necessary of any process that could lead to memory consolidation, which takes place over several hours (or overnight) after exposure to learning [28].

The networks affected by visuomotor adaptation, including the fronto-parietal (Figure 2) and cerebellar circuits (Figure 3), are known to be active during visuomotor adaptation [14, 15, 18–21] and are necessary for the long-term retention of motor skills [16, 17, 22]. In fact, there is a striking overlap between the areas identified with PICA in this experiment and areas involved in motor learning (see [29] for review) and areas that represent consolidated motor skills (see [30] for review).

Because a global cerebellar RSN has not been previously reported and because this component was not identified across the two groups during the baseline $REST_1$ session, it is important to scrutinize this result in greater detail. It may be the case that the learning task for the test group so strongly engaged this network in $REST_2$ (Figure 3B) that its increased strength after learning significantly contributed to the overall variability across *both* rest sessions. Hence we suggest that it has been identified only in the test group data because of its activation by learning. Previous imaging reports suggest widespread cerebellar activation during active performance of motor learning tasks [10, 12, 17], but as far as we are aware, no others have searched for cerebellar resting state components after a period of motor learning. In other words, global engagement of the cerebellum may not be typical during rest. Rather, its engagement may require recent cerebellum-dependent learning and its engagement would not be expected without such learning.

Activity within the resting brain may reflect the on-going "off-line" processing of information gained from earlier learning [8, 27, 31]. Short-term memories for past experiences are consolidated over time [31–35] and the processing and metabolic demands of consolidation must be met by the resting brain [8]. It is possible that these processes might also be reflected in the slow fluctuations of BOLD signal that are detected as RSNs. Moreover, consolidation processes would be expected to modulate the strength of cortico-cortical interactions [36], and thus be evident as the increase in strength of spatio-temporal patterns identified by PICA analysis. Thus, strengthening of PICA components, which indicates an increase in the proportion of BOLD signal variability explained by that component, may reflect greater correlated activity within the brain areas comprising the component. This was confirmed by correlational analysis briefly described above (see Supplemental Results) suggesting localized changes within these networks that will require additional research.

In conclusion, we have shown that motor learning, but not motor performance, can modulate particular resting state networks. This reveals a novel connection between neuroplasticity and subsequent resting state activity, which may in part arise because the off-line processing of memory during consolidation is supported by task-specific resting state activity. Our results add a new dimension to our understanding of the resting brain and potentially provide a powerful new technique to examine the neuronal machinery of off-line processing.

Experimental Procedures

Participants

We recorded BOLD signal from 24 right-handed participants over five consecutive conditions within a single scanning session (Figure 1A; see

Please cite this article in press as: Albert et al., The Resting Human Brain and Motor Learning, Current Biology (2009), doi:10.1016/j.cub.2009.04.028

Supplemental Experimental Procedures for full details). Participants were randomly assigned to either the test (6 men and 6 women; age: mean = 27.0 years, SEM = 2.77 years) or the control (5 men and 7 women; age: mean = 24.6 years, SEM = 1.39 years) group. Informed consent was obtained from each participant, and the experiment was approved by our local ethical committee. Participants received financial compensation for their time.

Behavioral Protocol

A 4 min dummy task immediately preceded each rest session, in which the participant passively viewed dynamic point light displays of human whole-body movements or scrambled versions that showed the same individual dot motions, but with random positions [37]. Individual stimuli lasted 3 s and were blocked into 30 s interleaved runs of 10 human and 10 scrambled motion stimuli. The participant was instructed to attend to the stimuli, discriminating human and scrambled movements, but had no active task to perform.

The visuomotor task [23] (see Supplemental Experimental Procedures) interleaved between the two rest sessions required the participants to use their nonpreferred left hand to move an MR-compatible joystick. In the test group, there was a novel angular displacement of 10° between the cursor and joystick position introduced every minute over 10 min, which produced a final 90° displacement. In the control group there was no novel relationship between the cursor and joystick position. Tracking performance was assessed in both groups by calculating the direction of the joystick with respect to the target during the first 100 ms of each movement, averaged across each block of 24 movements.

fMRI Analysis

Resting state analysis was carried out with PICA [26] as implemented by MELODIC (Multivariate Exploratory Linear Decomposition into Independent Components) Version 3.05, which is a part of FSL (Functional Magnetic Resonance Imaging of the Brain Software Library, http://www.fmrib.ox.ac.uk/fsl). Correlational analysis was performed with a GLM model within FEAT (FMRI Expert Analysis Tool, also within the FSL package). See Supplemental Experimental Procedures for further details.

Supplemental Data

Supplemental Data include Supplemental Results, Supplemental Experimental Procedures, three figures, and three tables and can be found with this article online at http://www.cell.com/current-biology/supplemental/S0960-9822(09)01026-4.

Acknowledgments

This work was supported by the Wellcome Trust (069439, R.C.M.) and by the U.S. National Institutes of Health (R01 NS051446, E.M.R.).

Received: December 8, 2008
Revised: April 3, 2009
Accepted: April 13, 2009
Published online: May 7, 2009

References

1. Raichle, M.E., MacLeod, A.M., Snyder, A.Z., Powers, W.J., Gusnard, D.A., and Shulman, G.L. (2001). A default mode of brain function. Proc. Natl. Acad. Sci. USA *98*, 676–682.
2. Fox, M.D., Snyder, A.Z., Vincent, J.L., Corbetta, M., Van Essen, D.C., and Raichle, M.E. (2005). The human brain is intrinsically organized into dynamic, anticorrelated functional networks. Proc. Natl. Acad. Sci. USA *102*, 9673–9678.
3. De Luca, M., Beckmann, C.F., De Stefano, N., Matthews, P.M., and Smith, S.M. (2006). fMRI resting state networks define distinct modes of long-distance interactions in the human brain. Neuroimage *29*, 1359–1367.
4. Damoiseaux, J.S., Rombouts, S., Barkhof, F., Scheltens, P., Stam, C.J., Smith, S.M., and Beckmann, C.F. (2006). Consistent resting-state networks across healthy subjects. Proc. Natl. Acad. Sci. USA *103*, 13848–13853.
5. Mantini, D., Perrucci, M.G., Del Gratta, C., Romani, G.L., and Corbetta, M. (2007). Electrophysiological signatures of resting state networks in the human brain. Proc. Natl. Acad. Sci. USA *104*, 13170–13175.
6. He, B.J., Snyder, A.Z., Zempel, J.M., Smyth, M.D., and Raichle, M.E. (2008). Electrophysiological correlates of the brain's intrinsic large-scale functional architecture. Proc. Natl. Acad. Sci. USA *105*, 16039–16044.
7. Raichle, M.E., and Snyder, A.Z. (2007). A default mode of brain function: A brief history of an evolving idea. Neuroimage *37*, 1083–1090.
8. Miall, R.C., and Robertson, E.M. (2006). Functional imaging: Is the resting brain resting? Curr. Biol. *16*, R998–R1000.
9. Baizer, J.S., Kralj-Hans, I., and Glickstein, M. (1999). Cerebellar lesions and prism adaptation in Macaque monkeys. J. Neurophysiol. *81*, 1960–1965.
10. Diedrichsen, J., Hashambhoy, Y., Rane, T., and Shadmehr, R. (2005). Neural correlates of reach errors. J. Neurosci. *25*, 9919–9931.
11. Doyon, J., Penhune, V., and Ungerleider, L.G. (2003). Distinct contribution of the cortico-striatal and cortico-cerebellar systems to motor skill learning. Neuropsychologia *41*, 252–262.
12. Miall, R.C., and Jenkinson, E.W. (2005). Functional imaging of changes in cerebellar activity related to learning during a novel eye-hand tracking task. Exp. Brain Res. *166*, 170–183.
13. Obayashi, S., Suhara, T., Kawabe, K., Okauchi, T., Maeda, J., Nagai, Y., and Iriki, A. (2003). Fronto-parieto-cerebellar interaction associated with intermanual transfer of monkey tool-use learning. Neurosci. Lett. *339*, 123–126.
14. Martin, T.A., Keating, J.G., Goodkin, H.P., Bastian, A.J., and Thach, W.T. (1996). Throwing while looking through prisms. I. Focal olivocerebellar lesions impair adaptation. Brain *119*, 1183–1198.
15. Clower, D.M., Hoffman, J.M., Votaw, J.R., Faber, T.L., Woods, R.P., and Alexander, G.E. (1996). Role of posterior parietal cortex in the recalibration of visually guided reaching. Nature *383*, 618–621.
16. Cohen, D.A., Pascual-Leone, A., Press, D.Z., and Robertson, E.M. (2005). Off-line learning of motor skill memory: A double dissociation of goal and movement. Proc. Natl. Acad. Sci. USA *102*, 18237–18241.
17. Imamizu, H., Miyauchi, S., Tamada, T., Sasaki, Y., Takino, R., Putz, B., Yoshioka, T., and Kawato, M. (2000). Human cerebellar activity reflecting an acquired internal model of a new tool. Nature *403*, 192–195.
18. Lee, J.H., and van Donkelaar, P. (2006). The human dorsal premotor cortex generates on-line error corrections during sensorimotor adaptation. J. Neurosci. *26*, 3330–3334.
19. Morton, S.M., and Bastian, A.J. (2004). Prism adaptation during walking generalizes to reaching and requires the cerebellum. J. Neurophysiol. *92*, 2497–2509.
20. Newport, R., Brown, L., Husain, M., Mort, D., and Jackson, S.R. (2006). The role of the posterior parietal lobe in prism adaptation: Failure to adapt to optical prisms in a patient with bilateral damage to posterior parietal cortex. Cortex *42*, 720–729.
21. Pisella, L., Rossetti, Y., Michel, C., Rode, G., Boisson, D., Pelisson, D., and Tilikete, C. (2005). Ipsidirectional impairment of prism adaptation after unilateral lesion of anterior cerebellum. Neurology *65*, 150–152.
22. Shadmehr, R., and Holcomb, H.H. (1997). Neural correlates of motor memory consolidation. Science *277*, 821–825.
23. Miall, R.C., Jenkinson, N., and Kulkarni, K. (2004). Adaptation to rotated visual feedback: A re-examination of motor interference. Exp. Brain Res. *154*, 201–210.
24. Baraduc, P., and Wolpert, D.M. (2002). Adaptation to a visuomotor shift depends on the starting posture. J. Neurophysiol. *88*, 973–981.
25. Tong, C., Wolpert, D.M., and Flanagan, J.R. (2002). Kinematics and dynamics are not represented independently in motor working memory: Evidence from an interference study. J. Neurosci. *22*, 1108–1113.
26. Beckmann, C.F., and Smith, S.M. (2004). Probabilistic independent component analysis for functional magnetic resonance imaging. IEEE Trans. Med. Imaging *23*, 137–152.
27. Peigneux, P., Orban, P., Balteau, E., Degueldre, C., Luxen, A., Laureys, S., and Maquet, P. (2006). Offline persistence of memory-related cerebral activity during active wakefulness. PLoS Biol. *4*, 647–658.
28. Robertson, E.M., Pascual-Leone, A., and Miall, R.C. (2004). Current concepts in procedural consolidation. Nat. Rev. Neurosci. *5*, 576–582.
29. Halsband, U., and Lange, R.K. (2006). Motor learning in man: A review of functional and clinical studies. J. Physiol. (Paris) *99*, 414–424.
30. Hazeltine, E., and Ivry, R.B. (2002). Motor skill. In Encyclopedia of the Human Brain, *Volume 3*, V.S. Ramachandran, ed. (San Diego, CA: Academic Press), pp. 183–200.
31. Robertson, E.M. (2009). From creation to consolidation: A novel framework for memory processing. PLoS Biol. *7*, e19.

Please cite this article in press as: Albert et al., The Resting Human Brain and Motor Learning, Current Biology (2009), doi:10.1016/j.cub.2009.04.028

32. Krakauer, J.W., and Shadmehr, R. (2006). Consolidation of motor memory. Trends Neurosci. *29*, 58–64.
33. Robertson, E.M., Pascual-Leone, A., and Press, D.Z. (2004). Awareness modifies the skill-learning benefits of sleep. Curr. Biol. *14*, 208–212.
34. Walker, M.P., Brakefield, T., Morgan, A., Hobson, J.A., and Stickgold, R. (2002). Practice with sleep makes perfect: Sleep-dependent motor skill learning. Neuron *35*, 205–211.
35. Brashers-Krug, T., Shadmehr, R., and Bizzi, E. (1996). Consolidation in human motor memory. Nature *382*, 252–255.
36. Diekelmann, S., and Born, J. (2007). One memory, two ways to consolidate? Nat. Neurosci. *10*, 1085–1086.
37. Jastorff, J., Kourtzi, Z., and Giese, M.A. (2006). Learning to discriminate complex movements: Biological versus artificial trajectories. J. Vis. *6*, 791–804.

Supplemental Data

The Resting Human Brain and Motor Learning

Neil B. Albert, Edwin M. Robertson, and R. Chris Miall

Supplementary Results

Behavioral Results

We assessed two additional features of the tracking movements, to test for non-specific changes in performance: the peak velocity of each outward movement and the latency of this moment from the onset of the target. The test group reached lower peak velocities (mean ± SEM: test = 2.16 ± 0.8°/s, control = 4.30 ± 0.8°/s; $F(1,20) = 368.12$, $p < 0.001$), but these occurred at a similar latency from the target onset in both groups (mean ± SEM: test = 731 ± 25ms, control = 701 ± 23ms; $F(1,20) < 1$). Critically, neither peak velocity nor its latency varied across the tracking session for either test or control groups (Group × Block interactions: $F(9,180) < 1$ in each case). In addition, the average directional errors of the control group were small and stable across the whole block (Figure 1B, main paper, grey solid line). Thus, the only indication of learning was in the initial direction of the joystick movements produced by individuals within the test group.

FMRI Results

Independent Components Analyses

To confirm that the component identified as modulated by learning (Figure 2, main paper) was also reliably identified in the pre-learning rest session, we concatenated the $REST_1$ data from the two participant groups into a single analysis. We identified a component (Supplementary Figure 1) that was very similar to the fronto-parietal component that was

modulated by motor learning in the test group (compare with Figure 2, main paper). The strength of this component was not significantly different between the two groups ($t(22) = 0.42$, $p = 0.68$). Thus this component was present in both groups initially, but was only affected by the visuo-motor task in the learning group.

Correlational Analyses

To verify our ICA analysis, we used ROI-based correlation analysis to calculate a mean covariance map for the $REST_1$ session across both groups (equivalent to the data shown in Supplementary Figure 1). A 5-mm region of interest was located in left superior frontal gyrus (xyz: -20, 26, 48), based on the local maximum coordinates in Supplementary Table 1. The correlation between BOLD signal in this ROI and all other voxels was calculated using a GLM analysis. As expected, the regions identified (Supplementary Figure 2) were close to those seen in the independent component analysis.

We then performed a 2x2 mixed effects ANOVA on correlational analyses for 5 seed ROIs, with group (test and control) and session ($REST_1$ vs $REST_2$) as factors. Significant positive or negative interactions were identified with uncorrected threshold of $p=0.001$ (Supplementary Table 3). Supplementary Table 3 indicates areas where the strength of correlation with these ROIS was significantly modulated by learning, as identified by significant interaction between the group (test vs control) and session ($REST_1$ vs $REST_2$) factors. Notable was a negative interaction between the left angular gyrus (xyz: -46, -70, 44) and the left hippocampus (Supplementary Figure 2) and positive interactions between left precentral gyrus (xyz: -42, 12, 44) and left middle frontal gyrus (BA45, Supplementary Figure 3A) and left inferior frontal cortex (BA47; Supplementary Figure 3B). These results confirm that the areas in which the correlation with the target region was significantly modulated by learning are largely

confined within the component identified by ICA, but also suggest that there is a complex intra-component network of correlations that will require detailed analyses to fully understand.

BOLD-behavior correlations

The change in strength of the two RSN components identified by PICA across participants within the test group (Figure 2, main paper) was not linearly correlated with behavioral measures of learning, but this does not imply there is no relationship. Our task instructions emphasized movement direction, rather than performance speed or terminal accuracy and so several different indices of learning might interact in defining the overall pattern of change in resting state activity [7, 8]. The gradual increase in the visuo-motor perturbation throughout the task was chosen to maximize adaptation to the task, but did not allow a clear measure of improved and retained skill. Additionally, there are between-subjects differences in baseline competence with our joystick, so we expect differences in learning rates across the group that may have no simple linear relationship with consolidation-related processing. Further investigation with much greater sample sizes and with assessments of individual differences before and after a training session will be necessary to fully address the quantitative relationship between behavioral measures of learning and changes in the resting brain.

Supplemental Experimental Procedures

Behavioral protocols

Participants were scanned throughout 5 consecutive sessions (Figure 1, main paper) taking a total of 45 minutes. The first was a 4 minute dummy task designed to ensure a common cognitive baseline, which immediately preceded each rest session. The participant passively viewed dynamic point light displays of human whole body movements, or scrambled versions that showed the same individual dot motions, but with random positions [1]. Individual stimuli

lasted 3s and were blocked into 30s interleaved runs of 10 human and 10 scrambled motion stimuli. The participant was instructed to attend to the stimuli, discriminating human and scrambled movements, but had no active task to perform.

The dummy task was followed by an 11-minute rest session, in which the participant was instructed to remain relaxed, with eyes closed. This was then followed by the visuo-motor task. Participants held the joystick case with their right hand and used their left hand to make small controlled movements of the joystick. Movements of the joystick tip of 1cm produced a 5.5cm on-screen cursor movement. Initially, visual feedback was veridical so that movement of the joystick towards the participant's feet elicited an upward movement of the cursor on the screen; left and right movements were veridical. A target appeared every 800 ms at one of 8 positions on a circle circumference centered on the start position, in pseudorandom order. After each 30 seconds (24 movements), target and cursor color changes cued participants to passively view the presented targets for 30 seconds. At the onset of the each successive active tracking block, in the test group the angular relationship between the joystick and cursor movement increased by 10° clockwise. Thus, the increasing visuomotor perturbation required test group participants to move the joystick counter-clockwise to the presented target on the screen, in order to direct the cursor towards the target. The cursor rotation increased by 10° each minute, throughout the 11 minute tracking task. For technical reasons, tracking data from the final block was lost for several participants. We therefore report tracking performance for only the first 10 blocks when the angular displacement in the test group had reached 90 degrees. Upon completion of the experiment, all participants expressed awareness of the existence of a visuo-motor perturbation.

Participants in the control group completed a very similar task to that described above. The only difference was that the angular relationship between the joystick and cursor movement

remained veridical throughout the 11 minute tracking task. An additional control group (n=14) completed the same adaptive task as the test group, but in the laboratory, and were then tested during the reintroduction of the veridical environment after the final adaptation block. This group showed the same level of adaptation as the test group, and also showed an aftereffect of 22° when returned to the veridical, unrotated condition, confirming learning.

The visuo-motor session was followed by another 4-minute dummy-task session, identical to the first, and was immediately followed by the second resting session, again identical to the first session. To additionally control for differences in mental state between the two rest sessions, other than learning, participants in both groups were falsely instructed that they would complete a second session of the tracking task after the second rest period. Thus both rest sessions were preceded by the same dummy task, and were undertaken in the expectation of a subsequent tracking task.

FMRI Acquisition.

218 T2*-weighted echo planar images (EPIs) were acquired using a 3T Philips Achieva scanner (Koninklijke Philips Electronics N.V., Eindhoven, Netherlands) during the resting and visuomotor blocks (TR =3 000ms; TE = 35ms; flip angle = 85°) using a SENSE head coil (SENSE factor 2). Each EPI volume was comprised of 49 96×96 axial slices of 2.5mm × 2.5mm × 3mm voxels, which covered the entire cerebral cortex and cerebellum (FOV = 240mm × 147mm × 240mm). A high-resolution T1-weighted structural volume (TR = 8.4ms; TE = 3.8ms; flip angle = 8°, FOV = 232mm × 288mm × 175mm) was also acquired for use during coregistration and normalization of the EPIs to the ICBM152-template [2] resliced to 2mm thick slices.

Independent Components Analyses

Independent analyses were run on each group, and the following procedures were followed for each of those analyses. The 24 EPI rest scans (218 volumes each) were concatenated in the model, along with a contrast model dissociating $REST_1$ sessions from $REST_2$ sessions. Thus, the PICA analysis would identify spatially consistent components across the 24 scans, without requiring common temporal structure. Each EPI volume was motion-corrected using MCFLIRT [3], high-pass filtered (0.01HZ cutoff), masked to eliminate non-brain voxels, spatially-smoothed using a 5mm FWHM filter, demeaned on a voxel-by-voxel basis, whitened, and projected into a 48-dimensional subspace using PICA. The dimensionality of the subspace was estimated using the Laplace approximation to the Bayesian evidence of the model order [4] for the test group, and set to 48 (the value from the approximation in the test group) for the control group. Non-brain structures were removed from the high-resolution structural image using BET [5] and the transformation matrix used for the affine registration of this image to the ICBM152 brain [2] was applied to the PICA output from each session.

The whitened observations were decomposed into sets of vectors which describe signal variation in the temporal domain (time-courses) across the spatial domain (maps) by optimizing for non-Gaussian spatial source distributions using a fixed-point iteration technique [6]. Estimated component maps once derived were used to generate an estimate of the error variance, which was used to convert the individual component maps into Z-score maps. These maps were then converted into probabilistic component maps by fitting the individual Z-score maps with Gamma/Gaussian Mixture-Models [4]. Components identified as reliably non-zero across the 24 scans were visually inspected to ensure that they were spatially similar to previously identified

resting networks, were not heavily influenced by any single scan, and contained limited power in frequencies above 0.1Hz. Each remaining component was tested using an ordinary least squares general linear model to find those that significantly differed in strength between the two REST sessions and were reliably non-zero across participants.

Correlational Analyses

Regions of interest were chosen based on the coordinates of local maxima within the main significant impendent component identified within fronto-parietal cortex (Figure 1, main paper). A 5mm radius spherical region was centered on each of 5 coordinates (see Table 1), and transformed into the original image space for each individual recording session (24 participants, 2 sessions). The mean BOLD signal within the ROI was then calculated from the preprocessed and filtered 4-D dataset for each data set. This temporal signal was used as a covariate for a whole-brain GLM analysis, in order to calculate the whole-brain covariance with the seed region. The 48 maps calculated for each of the 5 seed regions were then compared in a 2x2 mixed design, testing for significant group×session interactions. Positive interaction would identify areas where the correlation with the seed region was selectively enhanced after learning, whereas negative interactions would identify areas where there was a selective reduction in correlation,

References

1. Jastorff, J., Kourtzi, Z., and Giese, M.A. (2006). Learning to discriminate complex movements: biological versus artificial trajectories. Journal of vision 6, 791-804.
2. Mazziotta, J., Toga, A., Evans, A., Fox, P., Lancaster, J., Zilles, K., Woods, R., Paus, T., Simpson, G., Pike, B., et al. (2001). A probabilistic atlas and reference system for the human brain: International Consortium for Brain Mapping (ICBM). Philos. Trans. R. Soc. Lond. B. Biol. Sci. 356, 1293-1322.
3. Jenkinson, M., Bannister, P., Brady, M., and Smith, S. (2002). Improved optimization for the robust and accurate linear registration and motion correction of brain images. NeuroImage 17, 825-841.
4. Beckmann, C.F., and Smith, S.M. (2004). Probabilistic independent component analysis for functional magnetic resonance imaging. IEEE Trans. Med. Imaging 23, 137-152.
5. Smith, S.M. (2002). Fast robust automated brain extraction. Hum. Brain Mapp. 17, 143-155.
6. Hyvarinen, A. (1999). Fast and robust fixed-point algorithms for independent component analysis. IEEE Trans. Neural Networks 10, 626-634.
7. Diedrichsen, J., Hashambhoy, Y., Rane, T., and Shadmehr, R. (2005). Neural correlates of reach errors. J. Neurosci. 25, 9919-9931.
8. Hikosaka, O., Nakahara, H., Rand, M.K., Sakai, K., Lu, X., Nakamura, K., Miyachi, S., and Doya, K. (1999). Parallel neural networks for learning sequential procedures. Trends Neurosci. 22, 464-471.
9. Tzourio-Mazoyer, N., Landeau, B., Papathanassiou, D., Crivello, F., Etard, O., Delcroix, N., Mazoyer, B., and Joliot, M. (2002). Automated anatomical labeling of activations in SPM using a macroscopic anatomical parcellation of the MNI MRI single-subject brain. NeuroImage 15, 273-289.
10. Raichle, M.E., MacLeod, A.M., Snyder, A.Z., Powers, W.J., Gusnard, D.A., and Shulman, G.L. (2001). A default mode of brain function. Proc. Natl. Acad. Sci. USA 98, 676-682.
11. Fox, M.D., Snyder, A.Z., Vincent, J.L., Corbetta, M., Van Essen, D.C., Raichle, M.E (2005). The human brain is intrinsically organized into dynamic, anticorrelated functional networks. Proc. Natl. Acad. Sci. USA 102, 9673-9678.
12. De Luca, M., Beckmann, C.F., De Stefano, N., Matthews, P.M., and Smith, S.M. (2006). fMRI resting state networks define distinct modes of long-distance interactions in the human brain. NeuroImage 29, 1359-1367.

Table S1. Fronto-Parietal Network

Region	Volume mm^3	% Region	Mean Z	Peak Z	Peak x	y	z
Left Frontal Lobe							
*Superior Frontal Gyrus	22156	76	5.09	12.74	-20	26	48
Medial Superior Frontal Gyrus	18168	76	4.30	11.68	-10	38	44
Orbital Superior Frontal Gyrus	2923	38	2.82	5.42	-31	55	-3
Middle Frontal Gyrus	27159	70	4.72	13.02	-22	26	48
Orbital Middle Frontal Gyrus	5954	83	3.98	8.67	-42	46	-8
Orbital Inferior Frontal Gyrus	6687	49	3.16	8.59	-42	46	-9
Triangular Inferior Frontal Gyrus	12047	59	2.33	6.46	-42	22	32
*Opercular Inferior Frontal Gyrus	4470	54	3.00	7.62	-42	21	36
Supplementary Motor Area	4763	27	2.49	9.20	-11	26	52
*Precentral Gyrus	7088	25	2.75	7.64	-42	12	44
Left Parietal Lobe							
*Angular Gyrus	9127	98	5.76	8.81	-46	-70	44
Inferior Parietal Lobule	9730	50	3.43	7.88	-50	-55	37
Supramarginal Gyrus	1571	15	2.23	5.92	-55	-53	32
Superior Parietal Lobule	2529	15	1.43	4.80	-37	-69	51
Left Occipital & Temporal Lobes							
Lateral Occipital Gyri	5729	22	2.89	7.74	-49	-70	39
Middle Temporal Gyrus	11955	30	2.53	7.06	-46	-62	24
Inferior Temporal Gyrus	7826	30	2.07	5.44	-54	-42	-16
Right Frontal Lobe							
Superior Frontal Gyrus	9413	29	3.20	7.04	18	30	44
Medial Superior Frontal Gyrus	5480	32	2.56	5.98	12	42	40
Middle Frontal Gyrus	8322	20	2.19	7.03	22	34	44
Cerebellum							
*Crus II	6504	38	2.07	4.94	38	-74	-44

Supplementary Table 1. *The fronto-parietal network of the test group, identified across both rest sessions using PICA.*

The fronto-parietal network (Figure 2, main paper) engaged the left parietal and frontal lobes, and to a lesser extent, the left temporal lobe, the right frontal lobe and the right cerebellum. The table lists the volume of the identified component within each anatomical region defined by the AAL atlas [9], the percent of the AAL region covered by the component, the mean z-score of the component within the AAL region, the peak z-score and the coordinates of the peak. Five coordinates chosen for whole-brain correlation analyses are indicated by asterisks*.

Table S2. Cerebellar Network

Region	Volume mm^3	% Region	Mean Z	Peak Z	Peak x	y	z
Vermis							
Lobule 1 & 2	383	95	2.83	7.41	6	-45	-22
Lobule 3	1608	88	3.97	8.64	2	-34	-12
Lobule 4 & 5	3647	69	4.20	12.32	6	-58	-18
Lobule 6	2956	100	9.10	13.42	6	-62	-20
Lobule 7	1564	100	9.26	12.68	2	-62	-24
Lobule 8	1940	100	9.36	12.34	-2	-62	-26
Lobule 9	1276	93	6.96	10.31	2	-59	-34
Lobule 10	675	77	3.11	9.53	2	-51	-24
Left hemisphere							
Lobule 3	985	92	3.07	8.15	-4	-47	-20
Lobule 4 & 5	6984	77	3.64	11.50	-4	-61	-17
Lobule 6	13108	96	6.44	12.13	-14	-66	-24
Crus1	14521	70	3.18	10.71	-14	-67	-26
Crus2	10696	70	2.88	9.26	-4	-68	-29
Lobule 7b	2919	63	2.84	8.12	-6	-71	-35
Lobule 8	10625	70	3.28	11.48	-4	-62	-29
Lobule 9	4946	71	2.45	8.39	-6	-56	-34
Lobule 10	719	62	1.42	6.34	-26	-41	-40
Right hemisphere							
Lobule 3	1212	76	2.77	8.90	7	-47	-20
Lobule 4 & 5	4857	72	3.25	12.63	8	-57	-20
Lobule 6	12996	90	6.50	13.60	10	-58	-20
Crus1	13452	64	2.97	9.82	14	-74	-25
Crus2	9383	55	2.05	10.42	5	-67	-28
Lobule 7b	2561	61	2.31	8.90	10	-72	-40
Lobule 8	13202	72	3.57	10.89	5	-63	-28
Lobule 9	4765	74	2.65	9.14	9	-56	-36
Lobule 10	528	41	1.06	5.57	26	-38	-40

Supplementary Table 2. *The cerebellar network for the test group across both rest sessions.*
A single IC component covered much of the bilateral cerebellum (Figure 3, main paper). Above are the sub-volumes of the component within each anatomically (AAL) defined cerebellar region, the percent of the region covered by the component, the mean z-score within the region, the peak z-score within each region, and the location of the region's peak activation. This component was not identified in the analysis of the control group.

Table S3. Correlation Analysis

Seed ROI	Volume mm^3	Peak Z	Peak location x	y	z
1 Superior frontal gyrus					
Negative interaction					
L Fusiform cortex	40	3.413	-44	-18	-20
2 Opercular inferior frontal gyrus					
Positive interaction					
L Middle frontal gyrus	64	3.627	-40	28	34
Negative interaction					
L Cerebellum lobule IX	8	3.502	-6	-48	-52
3 Precentral gyrus					
Positive interaction					
L Middle frontal gyrus	144	3.989	-40	28	30
L Inferior frontal gyrus	72	3.402	-42	44	-8
Negative interaction					
L Cerebellum, crus I	8	3.14	-42	-70	-20
4 Angular gyrus					
Positive interaction					
L Inferior temporal gyrus	24	3.163	-56	-38	-16
Negative interaction					
L Hippocampus	128	3.63	-26	-28	-8
5 Cerebellar Crus II					
Positive interaction					
L Brainstem, Pons	8	3.150	-14	-30	-32

Supplementary Table 3. *The areas with significant group(test and control)×session (Rest 1 vs Rest 2) interaction in strength of correlation with regions of interest (ROIs) identified in Table 1.* The 2×2 ANOVA was used to find areas with significant interaction between group and session that demonstrate a learning-dependent change in correlation between the seed ROI and all other brain areas. For each of 5 seed ROIs, areas that were statistically significant for either the positive and negative interactions (p=0.001 uncorrected) are shown.

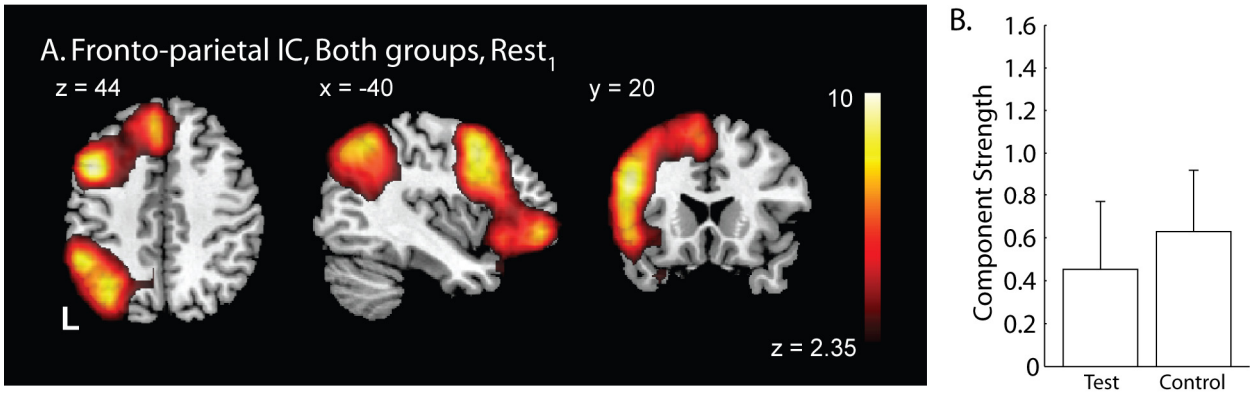

Figure S1. *The fronto-parietal component identified by PICA, which increased in strength following motor skill learning, is similar in strength prior to motor performance or motor learning in the test and control groups, respectively.* The component shown in panel A was reliable across the participants in both groups during the initial rest. The strength of the component did not vary between groups (panel B). This component includes the same areas as those in the initial analysis of the test group (see Supplementary Table 1), but includes a broader region within the right hemisphere of the cerebellum (not shown).

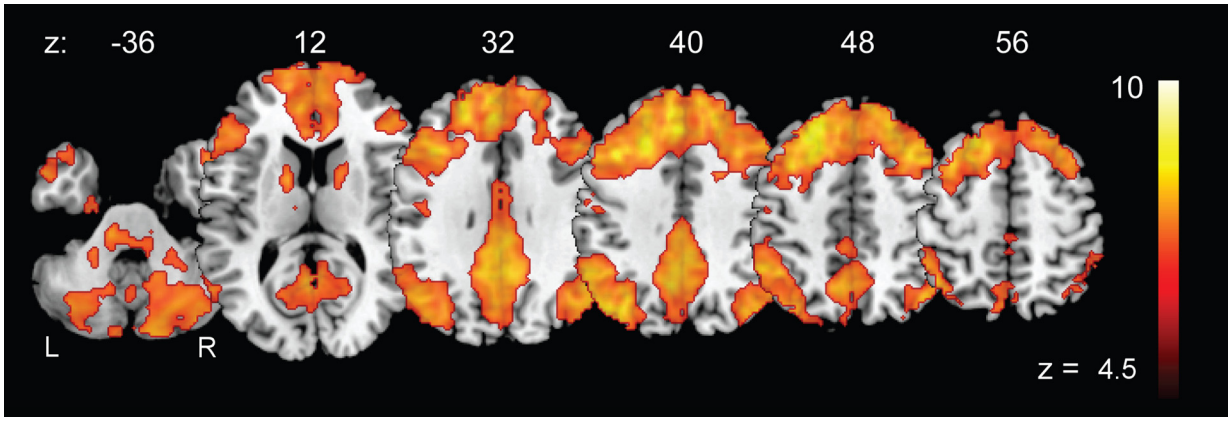

Figure S2. *Regions correlated with the left superior frontal gyrus seed.* The BOLD signal recorded during both sessions within the regions shown were significantly correlated with the activity in a seed region of interest centered on the superior frontal gyrus (Table 1, ROI 1), in both participant groups. The strength of the correlation did not significantly vary between groups. This component includes the same areas as those identified using PICA analysis (Supplementary Figure 1) but also includes a broader bilateral frontal region and a noticeable region within the medial parietal cortex, as frequently observed in default state analyses [10-12].

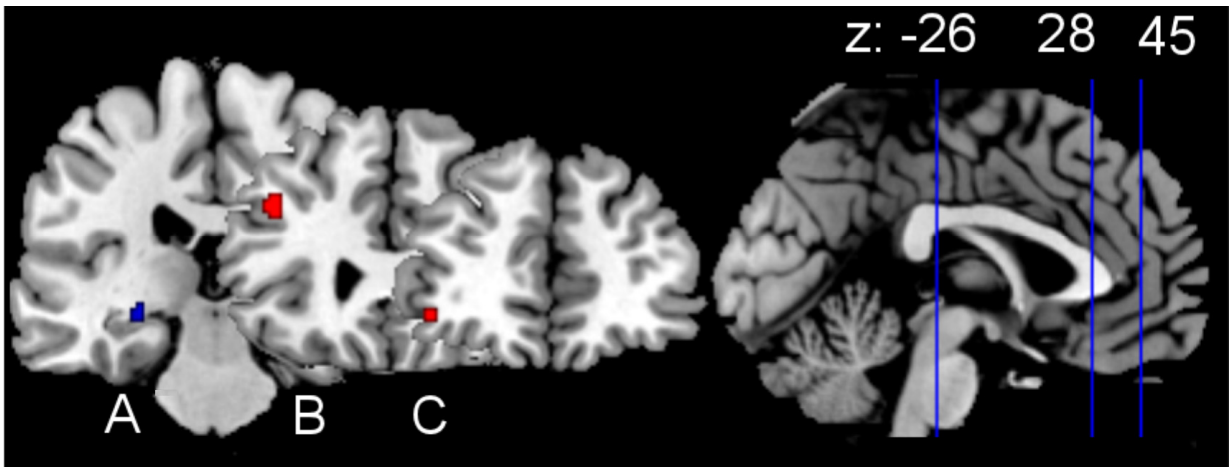

Figure S3. *Some of the areas significantly correlated with regions of interest centered on the precentral gyrus (red) or the angular gyrus (blue) (see Supplementary table 3, ROIs 3 and 4).* The regions were correlated with activity in the seed regions and the strength of the correlation was significantly increased (red) or decreased (blue) by learning – hence these areas showed a significant positive or negative group (test and control) ×session ($REST_1$ 1 vs $REST_2$) interaction in strength of correlation, respectively. The area in blue (A) is in the left hippocampus; red areas are in left middle (B: BA45) and inferior frontal gyri (C: BA47).